

Self-regulation in self-propelled nematic fluids

A. Baskaran^{1,a} and M.C. Marchetti²

¹ Martin Fisher School of Physics, Brandeis University, Waltham, MA, USA

² Physics Department and Syracuse Biomaterials Institute, Syracuse University, Syracuse, NY 13244, USA

Received 15 April 2012 and Received in final form 8 July 2012

Published online: 28 September 2012 – © EDP Sciences / Società Italiana di Fisica / Springer-Verlag 2012

Abstract. We consider the hydrodynamic theory of an active fluid of self-propelled particles with nematic aligning interactions. This class of materials has polar symmetry at the microscopic level, but forms macrostates of nematic symmetry. We highlight three key features of the dynamics. First, as in polar active fluids, the control parameter for the order-disorder transition, namely the density, is dynamically convected by the order parameter via active currents. The resulting dynamical self-regulation of the order parameter is a generic property of active fluids and destabilizes the uniform nematic state near the mean-field transition. Secondly, curvature-driven currents render the system unstable deep in the nematic state, as found previously. Finally, and unique to self-propelled nematics, nematic order induces local polar order that in turn leads to the growth of density fluctuations. We propose this as a possible mechanism for the smectic order of polar clusters seen in numerical simulations.

1 Introduction

Active materials are soft materials driven out of equilibrium by energy input at the microscale. This liberates the fluctuations from the constraints of equilibrium such as fluctuation-dissipation relations and reciprocity. As a consequence, several exotic emergent behaviors result, such as long-range order in 2D [1, 2], anomalous fluctuations [3, 4], dynamical structures and patterns [5–8]. In addition to serving as prototypical systems to explore emergent dynamical behavior, active materials also form the physical scaffold of biological systems in that active matter, when coupled to regulatory signaling pathways, provides a model for a variety of living systems, such as bacterial biofilms or the cytoskeleton of a cell.

Active particles are generally elongated and form orientationally ordered states [9]. The nature of the ordered state depends on both the symmetry of the individual particles and the symmetry of the aligning interactions (see fig. 1). Physical realizations of *polar* active particles (with distinct head and tail) include bacteria, asymmetric vibrated granular rods, and polarized migrating cells. Polar active entities are often modeled as self-propelled (SP) particles, where the activity is incorporated via a self-propulsion velocity of the individual entities. *Apolar* (head-tail symmetric) active particles, often referred to as “shakers”, have also been considered in the literature. Realizations are symmetric vibrated rods [4]. It has also been

argued that melanocytes, the cell that distribute pigments in our skins, may effectively behave as “shakers” [10, 11].

The nature of the interaction is of course crucial in controlling the properties of the ordered state. SP and polar particles may experience either polar interactions, *i.e.*, ones that tend to align particles head to head and tail to tail, or interactions that are apolar, *i.e.*, align particles regardless of their polarity. Well studied examples of polar particles with polar interactions are provided by Vicsek-type models [12, 13]. This class of active systems, referred to below as *active polar* fluids, can order in polar states, characterized by a nonzero vector order parameter and mean motion. Apolar active particles (shakers) generally experience apolar interactions and the resulting ordered state has the symmetry of equilibrium nematic liquid crystals. The broken orientational symmetry identifies a direction $\hat{\mathbf{n}}$, but the ordered state is invariant for $\hat{\mathbf{n}} \rightarrow -\hat{\mathbf{n}}$. These systems will be called *active nematic* fluids in the following. Their properties have been studied by several authors [3, 14]. One can envisage another class of active fluids with nematic symmetry at large scales that consists of SP particles (hence units that are polar at the micro scale) with apolar aligning interactions. A realization of this is self-propelled particles with physical interactions, such as steric repulsion or hydrodynamic couplings among swimmers in a bulk suspension. It has been shown that these interactions lead to large-scale nematic, rather than polar order [15, 16]. What is key is the fact that binary interactions such as steric collisions or hydrodynamic couplings individually conserve momentum and hence cannot

^a e-mail: aparna@brandeis.edu

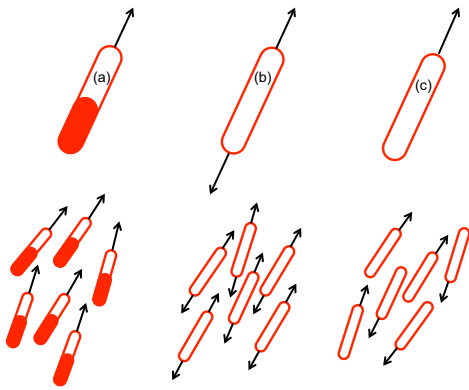


Fig. 1. Top: active particles of various microscopic symmetry: (a) Polar active particles with head/tail asymmetry resulting in polar interactions, as studied in [12, 13]. (b) Apolar active particles, as studied in [3, 14]. (c) Self-propelled particles, with physical head-tail symmetry, resulting in apolar interactions. Bottom: ordered macroscopic states of active particles: polar active fluid (left) formed by polar particles (a) with polar interactions; active nematic fluid (center) formed by apolar particles (b) with apolar interactions; self-propelled active nematic fluid (right) formed by self-propelled particles (c) with apolar interactions.

lead to the development of a macroscopic momentum for the system. Since the ordered state of these systems has nematic symmetry, the reader may wonder why we feel the need to group these active fluids in a separate (third) class. The reason is that, as we will see below, the properties of active nematic of SP particles are distinct from those of active nematics composed of apolar particles. We will refer to this third class of active systems as *self-propelled nematic* fluids. Further, it has recently become apparent that models of polar particles with apolar interactions may be relevant to a number of physical systems, including gliding myxobacteria [17], suspensions of auto-catalytic Janus colloids [18] and motile epithelial cell sheets such as those studied in wound healing assays [19, 20]. Self-propelled nematics therefore represent an important new class of active systems of direct experimental relevance.

A useful theoretical framework for describing the collective behavior of active systems is a continuum model that generalizes liquid crystal hydrodynamics to include new terms induced by activity [14, 21–29]. In this paper, we discuss the hydrodynamics of active fluids of nematic symmetry, contrasting the behavior of fluids composed of shakers and of self-propelled particles. We consider minimal continuum models based on the equations derived earlier by us from specific microscopic models [15, 30], but in contrast to our previous work, here we introduce the models phenomenologically on pure symmetry grounds. We also use the present paper to clarify some apparent discrepancies between our earlier publications. In our previous work we considered collections of repulsive hard rods self-propelled at speed v_0 along their long axis, and discussed two different ways of implementing the steric in-

teractions. In ref. [30] we described the hard rod interaction within the Onsager mean-field model of excluded volume, neglecting any modification that self-propulsion may induce to the hard rod collision. In contrast, in ref. [15] we analyzed in details the collision of two self-propelled hard rods and showed that self-propulsion enhances longitudinal momentum transfer and yields new nonequilibrium terms in the continuum equations not obtained in the mean-field Onsager model. We show here that the equations obtained in ref. [30] can be recast in the form of the equations used in the literature [3] to describe collections of shakers. The large-scale dynamics of this system that we call *active nematic*, like that of its equilibrium counterpart, can therefore be described solely in terms of density and alignment tensor, albeit with active currents not present in the equilibrium equations. In contrast, the description of the dynamics of *self-propelled nematics* requires the inclusion of an additional collective velocity or polarization field. Further, we show that *all* active fluids with large-scale nematic symmetry (both consisting of shakers and SP particles) exhibit the phenomenon of dynamical self-regulation [31], due to the fact that the parameter controlling the order-disorder transition, namely the density ρ of active particles, is not externally tuned, as in systems undergoing equilibrium phase transitions, but it is dynamically coupled to the order parameter. This coupling is analogous to the one present in polar fluids [1, 2, 32] and is a generic mechanism for emergent structure in all active systems, as demonstrated in our recent work [31].

The layout of the paper is as follows. First, we construct the hydrodynamic description of active fluids with nematic symmetry, highlighting the difference between self-propelled particles with an equilibrium-like aligning interaction, unmodified by self-propulsion (such as the Onsager excluded-volume description of the steric repulsion of two hard rods), and the case where the binary collision is modified by self-propulsion. In the former case the system is equivalent at large scales to an active nematic of shakers, while the second case corresponds to a new class of self-propelled nematic fluids. Next we examine the linear stability of the homogeneous nematic state. We show that there exists three dynamical mechanisms responsible for emergent structures in active fluids with nematic symmetry. The first is a model-independent instability that occurs in the vicinity of the mean field order disorder transition due to the coupling between order parameter and mass transport which renders the dynamics of the system self-regulating. We argue that this instability is the basis for the emergence of bands and phase separation found ubiquitously active systems [33–35]. The second is the well known instability of director fluctuations that arises from nonequilibrium curvature-induced fluxes and is closely related to the giant number fluctuations observed in these systems [3, 14]. These two instabilities are common to both active nematics and self-propelled nematics, *i.e.*, occur regardless of the symmetry of the microdynamics. Finally, we show that there exists a third instability unique to self-propelled nematic fluids due to the fact that in these systems, large scale nematic order

can induce local polar order, which in turn destabilizes the density. This mechanism may be responsible for the smectic order of polar clusters observed recently in simulations of SP rods [34, 36]. We conclude with a brief discussion.

2 The macroscopic theory

The hydrodynamic equations of a self-propelled nematic have been derived from systematic coarse-graining of specific microscopic models [15, 16, 30]. Here we introduce these equations phenomenologically, with the goal of examining the dynamics without the limitations imposed by the specific parameter values obtained from a microscopic model or resulting from the choice of the closure used in the kinetic equation.

We limit ourselves to overdamped systems in two dimensions. The hydrodynamic equations are then written in terms of three continuum fields: the conserved number density $\rho(\mathbf{r}, t)$ of active units, the polarization density $\boldsymbol{\tau}(\mathbf{r}, t) = \rho(\mathbf{r}, t)\mathbf{P}(\mathbf{r}, t)$, with $\mathbf{P}(\mathbf{r}, t)$ a polarization order parameter, and the nematic alignment density tensor $Q_{ij}(\mathbf{r}, t) = \rho(\mathbf{r}, t)S_{ij}(\mathbf{r}, t)$. The polarization \mathbf{P} is directly proportional to the collective velocity of the active particles, while S_{ij} is the conventional nematic order parameter tensor familiar from liquid crystal physics. For a uniaxial system in two dimensions, Q_{ij} is a symmetric traceless tensor with only two independent components and can be written in terms of a unit vector $\hat{\mathbf{n}}$ as $Q_{ij} = Q(\hat{n}_i\hat{n}_j - \frac{1}{2}\delta_{ij})$, where $Q = \rho S$; S is the magnitude of the order parameter and the director $\hat{\mathbf{n}}$ identifies the direction of spontaneously broken symmetry in the nematic state. For simplicity most of the discussion below refers to the case where the active particles are modeled as long thin rods with repulsive interactions.

2.1 Active nematic hydrodynamics

We first discuss the hydrodynamic equations of a collection of nematic rods self-propelled along their long axis obtained, as in ref. [30], by incorporating the advective terms due to self-propulsion, but assuming that self-propulsion does not modify the hard rod interactions. This model corresponds for instance to the one studied numerically in [33]. The hydrodynamic equations for this system can be written in two different forms corresponding in a microscopic model to different closures of the kinetic equation. These two forms can be shown to be equivalent at long times. First, one could write a set of coupled equations for density, polarization and alignment tensor, given by

$$\partial_t \rho + v_0 \nabla \cdot \boldsymbol{\tau} = D \nabla^2 \rho, \quad (1a)$$

$$\partial_t \boldsymbol{\tau} + D_r \boldsymbol{\tau} + v_0 \nabla \cdot \mathbf{Q} + \frac{v_0}{2} \nabla \rho = D_\tau \nabla^2 \boldsymbol{\tau}, \quad (1b)$$

$$\begin{aligned} \partial_t Q_{ij} - D_r [\alpha(\rho) - \beta \mathbf{Q} : \mathbf{Q}] Q_{ij} + \frac{v_0}{4} F_{ij} = D_b \nabla^2 Q_{ij} \\ + D_s \partial_k (\partial_i Q_{kj} + \partial_j Q_{ik} - \delta_{ij} \partial_l Q_{kl}), \end{aligned} \quad (1c)$$

where $\mathbf{Q} : \mathbf{Q} = Q_{kl} Q_{kl}$, D_r is the rotational diffusion rate and $F_{ij} = (\partial_i \tau_j + \partial_j \tau_i - \delta_{ij} \nabla \cdot \boldsymbol{\tau})$. All terms proportional to v_0 arise from one-particle convection due to self-propulsion and are the only consequence of activity in this simple model that assumes equilibrium-like interactions. The repulsive interactions among the particles generate the cubic homogeneous term (with $\beta > 0$) on the right hand side of eq. (1c) and a change in sign of $\alpha(\rho) \sim \rho - \rho_c$ at a critical density ρ_c , controlling the transition between the isotropic and the nematic states¹. Interactions also give density-dependent corrections to the various diffusion coefficients for density (D), polarization (D_τ), splay (D_s) and bend (D_b) deformations of the nematic alignment tensor. We will ignore all such corrections in the following². Finally, for simplicity here and below, unlike what done in refs. [15, 30], we have assumed equal splay and bend elastic constants in the polarization equation.

Since in this system the interactions are purely nematic and identical to those of an equilibrium system, the polarization decays on short time scales of order D_τ^{-1} for all strengths of self-propulsion speed. One can therefore neglect $\partial_t \boldsymbol{\tau}$ in eq. (1b) relative to $D_r \boldsymbol{\tau}$ and eliminate the polarization $\boldsymbol{\tau}$ in favor of density and alignment tensor, with the result

$$\partial_t \rho = D \nabla^2 \rho + D_Q \nabla \nabla : \mathbf{Q}, \quad (2a)$$

$$\begin{aligned} \partial_t Q_{ij} - D_r [\alpha(\rho) - \beta \mathbf{Q} : \mathbf{Q}] Q_{ij} = D_b \nabla^2 Q_{ij} \\ + D_s \partial_k (\partial_i Q_{kj} + \partial_j Q_{ik} - \delta_{ij} \partial_l Q_{kl}) \\ + D_\rho \left(\partial_i \partial_j - \frac{1}{2} \delta_{ij} \nabla^2 \right) \rho. \end{aligned} \quad (2b)$$

The active currents proportional to D_Q and D_ρ are unique to non-equilibrium systems (with $D_Q, D_\rho \sim v_0^2$ in the present model) and vanish in equilibrium. The reader may be confused by the fact that ref. [30] reported coupled equations for density, alignment tensor *and* polarization, and yet included the active currents absent in eqs. (1). The reason for this discrepancy is that ref. [30] used a specific low density approximation that does give a finite value for the coefficients of these nonequilibrium currents. These currents would, however, vanish if their coefficients were to be calculated exactly to all order in the density³, showing that active modifications of nematic interactions (such as excluded volume) are needed to yield nonzero values of D_Q and D_ρ .

The term proportional to D_Q is the curvature-induced density flux that has been discussed extensively by Ra-

¹ Note that the cubic term was not derived in ref. [30], but is easily obtained, including its sign, by a higher order closure of the moment expansion of the kinetic equation.

² Retaining the density dependence of the diffusion coefficients results in interesting emergent structures as shown by [37]. Since we seek to focus on fundamental features that do not depend on the detailed structure of the hydrodynamic coefficients, we ignore this physically important feature.

³ A hint to this is obtained by looking at the excluded-volume corrections given in the appendix of ref. [30].

maswamy and collaborators [3] and shown to be responsible for giant number fluctuations in the ordered state of active nematic. The diffusive coupling proportional to D_ρ describes similar physics but has not been considered in earlier description of active nematic fluids. In addition, activity also yields corrections to the various diffusion coefficients. We have, however, implicitly neglected those here by retaining the same notation for these quantities as in eqs. (1a)-(1c) to highlight the difference between these corrections that do not change the dynamics qualitatively and the new terms proportional to D_Q and D_ρ . Although obtained here by considering a system of self-propelled particles, eqs. (2a) and (2b) have the same structure as the hydrodynamic equations of an active nematic, consisting of a collection of *apolar* active particles (shakers) with apolar interactions. This is an important point as it stresses that the qualitative differences between active and self-propelled nematic that have been observed in simulations must arise entirely from the dependence of the interaction on self-propulsion v_0 .

2.2 Momentum-conserving interaction of self-propelled nematogens

As shown in ref. [15] and supported by simulations of self-propelled hard rods [34–36, 38], self-propulsion does modify the repulsive interaction in a qualitative way. This modification results in local build-up of polarization in the nematic state, making it necessary to retain the dynamics of polarization density in the continuum model. The modification of the Onsager excluded-volume interactions among hard rods due to self-propulsion is worked out in ref. [39]. Here we simply give a qualitative description of this effect and we refer the reader to that work for the technical details. First we note that the presence of a self-propulsion speed along the long axis of the nematogen, results in a breaking of the nematic symmetry of the microdynamics, as shown in fig. 1. On the other hand, since the interactions conserve momentum, this cannot lead to a macroscopic breaking of polar symmetry as this would amount to the appearance of a spontaneous macroscopic momentum from a zero momentum state. Hence, only a homogeneous ordered nematic state can occur and the associated mean field transition will be the same as in the case of the active nematic considered above, albeit with coefficients α and β renormalized by self-propulsion [15]. Even though the polar symmetry cannot be broken macroscopically, momentum conservation allows the nematic ordering to induce local polar order in the system. To illustrate this, let us consider hard rods in two dimensions undergoing energy-momentum conserving interactions. As shown in fig. 2, the angular momentum transfer due to the linear momentum from self-propulsion for a collision between two rods scales as $\omega \sim \cos(\theta_1 - \theta_2) \sin(\theta_1 - \theta_2)$. If the rods are nearly aligned head to head (as in fig. 2a), the effect of this angular momentum is to turn the rods towards each other, while if they are nearly aligned head to tail as in fig. 2b, the collision turns both rods in the same direction, leaving their relative angle unchanged. This mech-

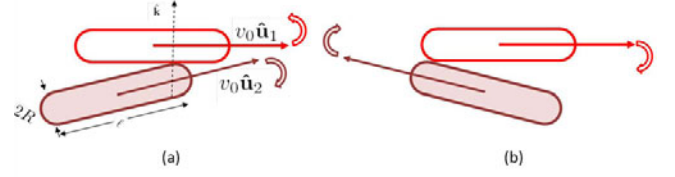


Fig. 2. Qualitative illustration of momentum-conserving collisions among self-propelled particles. It can readily be shown that two rods as shown in (a), coming in with only their self-replenishing velocities, will acquire opposite angular momenta $\omega_1 \sim \hat{z} \ell v_0 [\hat{z} \cdot (\hat{\mathbf{u}}_1 \times \hat{\mathbf{u}}_2)]$ and $\omega_2 \sim -\hat{z} \ell v_0 (\hat{\mathbf{u}}_1 \cdot \hat{\mathbf{u}}_2) [\hat{z} \cdot (\hat{\mathbf{u}}_1 \times \hat{\mathbf{u}}_2)]$, where the vectors are defined in the image and in [39]. The collision will therefore induce rotations as indicated, promoting alignment of the two rods. On the other hand, two nearly anti-aligned rods as in (b) acquire angular momenta of the same sign, inducing rotation of both rods in the same directions, and leaving their relative angle nearly unchanged.

anism effectively promotes head-to-head alignment. Since collisions among such nearly aligned nematogens will dominate the dynamics in the nematic state, the nematic order effectively induces polar order.

2.3 Self-propelled nematic hydrodynamics

The fact that interactions among self-propelled nematogens tend to induce polar order is reflected in the hydrodynamic description by a number of new nonlinear terms that couple τ and \mathbf{Q} , with coefficients that vanish in the limit $v_0 = 0$. The continuum equations for a self-propelled nematic that incorporate the above physics are given by

$$\partial_t \rho + v_0 \nabla \cdot \tau = D \nabla^2 \rho + D_Q \nabla \nabla : \mathbf{Q}, \quad (3a)$$

$$\begin{aligned} \partial_t \tau + D_r \tau + \gamma_1 \mathbf{Q} : \mathbf{Q} \tau - \gamma_2 \tau \cdot \mathbf{Q} + \lambda_1 \tau \cdot \nabla \tau = \\ -v_0 \nabla \cdot \mathbf{Q} - \frac{v_0}{2} \nabla \rho + \lambda_2 \tau \nabla \cdot \tau + \frac{\lambda_3}{2} \nabla \tau^2 + D_\tau \nabla^2 \tau, \end{aligned} \quad (3b)$$

$$\begin{aligned} \partial_t Q_{ij} - D_r (\alpha - \beta \mathbf{Q} : \mathbf{Q}) Q_{ij} + \frac{v_0}{4} F_{ij} + \lambda_4 G_{ij} = \\ D_s \partial_k (\partial_i Q_{kj} + \partial_j Q_{ik} - \delta_{ij} \partial_l Q_{kl}) \\ + D_\rho \left(\partial_i \partial_j - \frac{\delta_{ij}}{2} \nabla^2 \right) \rho + D_b \nabla^2 Q_{ij}, \end{aligned} \quad (3c)$$

where $G_{ij} = Q_{ik} \partial_k P_j + Q_{jk} \partial_k P_i - \delta_{ij} Q_{kl} \partial_k P_l$ and again we have implicitly neglected active corrections to D , D_τ , D_s and D_b to highlight the new, purely active terms. Equations (3) are of the form given in ref. [15] (but note that in [15] we had omitted the $\mathcal{O}(\nabla^2)$ splay and bend terms in the equation for the alignment tensor), with one important exception: the term proportional to γ_1 was not obtained in our earlier work where a closure that only retained terms up to quadratic in the continuum fields was used to derive the hydrodynamic equations. This cubic term is, however, allowed by symmetry and does indeed arise from the microscopic model discussed in [15] if a higher order closure of the kinetic equation is used to derive hydrodynamics. As shown below, it has important consequences for pattern

formation as it drives the built-up of local polar order. Activity enters in eqs. (3) through the convective terms proportional to v_0 , the new terms with coefficients γ_i and λ_i , which vanish in equilibrium, as well as the terms proportional to \mathcal{D}_Q and \mathcal{D}_ρ that arise here from active corrections to interactions. Finally, the parameters α and β controlling the mean field isotropic-nematic transition are also renormalized by activity. The homogeneous nonlinearities proportional to γ_i in the polarization equation encode the fact that nematic order induces polar order. The latter is, however, only local as the equations do not admit a homogeneous solution with nonzero $\boldsymbol{\tau}$. Further, the active modification of the interactions, yield the convective nonlinearities $\sim \mathcal{O}(\boldsymbol{\tau}\nabla\boldsymbol{\tau})$ that play a central role in the emergent physics of active polar fluids.

Since the goal of this presentation is to highlight the mechanisms responsible for emergent structures, we simplify the equations by setting all of the equilibrium-like diffusion coefficients to be equal, *i.e.*, $D = D_\tau = D_b = D_0$, with the exception of the splay relaxation constants D_s . In addition, we assume $\lambda_i = \lambda$ for all i 's and $\gamma_1 = \gamma_2 = \gamma$ (in their nondimensional forms). Finally, we measure time in units of $1/D_r$ and lengths in units of $\sqrt{D_0/D_r}$. The hydrodynamic equations then simplify to (in nondimensional form)

$$\partial_t \rho + \bar{v} \nabla \cdot \boldsymbol{\tau} = \nabla^2 \rho + \bar{D}_Q \nabla \nabla : \mathbf{Q}, \quad (4a)$$

$$\begin{aligned} \partial_t \boldsymbol{\tau} + (1 + \gamma \mathbf{Q} : \mathbf{Q}) \boldsymbol{\tau} - \gamma \boldsymbol{\tau} \cdot \mathbf{Q} + \lambda \boldsymbol{\tau} \cdot \nabla \boldsymbol{\tau} = \\ - \bar{v} \nabla \cdot \mathbf{Q} - \frac{\bar{v}}{2} \nabla \rho + \lambda \left(\boldsymbol{\tau} \nabla \cdot \boldsymbol{\tau} + \frac{1}{2} \nabla \tau^2 \right) + \nabla^2 \boldsymbol{\tau}, \end{aligned} \quad (4b)$$

$$\begin{aligned} \partial_t Q_{ij} - (\alpha - \beta \mathbf{Q} : \mathbf{Q}) Q_{ij} + \bar{v} F_{ij} + \lambda G_{ij} = \\ \bar{D}_\rho \left(\partial_i \partial_j - \frac{1}{2} \delta_{ij} \nabla^2 \right) \rho \\ + \bar{D}_s \partial_k (\partial_i Q_{kj} + \partial_j Q_{ik} - \delta_{ij} \partial_l Q_{kl}) + \bar{D}_b \nabla^2 Q_{ij}, \end{aligned} \quad (4c)$$

with $\bar{D}_Q = \mathcal{D}_Q/D_0$, $\bar{D}_\rho = \mathcal{D}_\rho/D_0$ and $\bar{D}_{s,b} = D_{s,b}/D_0$. Finally, we assume $\alpha = \frac{\rho}{\rho_c} - 1$ and β independent of ρ . The effect of activity is assumed to affect the mean field phase transition only through the dependence of the critical density ρ_c on the magnitude of self-propulsion speed. In this simplified form, the dynamics of the system is characterized by two central parameters: the mean density ρ_0 of active nematogens and the self-propulsion velocity $\bar{v} = v_0/\sqrt{D_r D_0}$, which is effectively the Peclet number for this flow. The other parameters γ , λ , \bar{D}_Q , \bar{D}_ρ and \bar{D}_s are in general functions of ρ_0 and \bar{v} , although we will treat them here as independent parameters and simply fix their values.

3 Linear dynamics and emergent structures

The dynamics of self-propelled rod-like particles with steric repulsion has been studied extensively by numerical simulation of microscopic models [34, 36, 38]. This work has revealed a rich variety of emergent structures, including bands of high density regions where the particles are

ordered along the direction of the band, lane formation, migrating defect structures and low Reynolds number turbulence. Here we examine the minimal continuum model of self-propelled nematic given by eqs. (4) to identify the generic dynamical mechanisms responsible for the emergence of these structures. As mentioned above, there are three important mechanisms for dynamical instabilities and pattern formation in these systems. To unfold the role of each of these mechanisms in controlling the large-scale dynamics of the system, we analyze the linear stability of the ordered nematic state in various special cases that best highlight a particular mechanism.

The ordered nematic state has constant density ρ_0 , zero mean polarization density, $\boldsymbol{\tau}_0 = 0$, and a finite value for the nematic alignment tensor. Choosing a coordinate system with the x axis pointing along the direction of broken nematic symmetry, the alignment tensor in the uniform nematic state has components $Q_{xx}^0 = -Q_{yy}^0 = Q_0/2$ and $Q_{xy}^0 = Q_{yx}^0 = 0$, with $Q_0 = \sqrt{\alpha_0/\beta}$ and $\alpha_0 = \alpha(\rho_0)$. We now examine the linear stability of this state in various regions of parameters by considering the dynamics of small fluctuations, $\delta\rho(\mathbf{r}, t) = \rho(\mathbf{r}, t) - \rho_0$, $\delta\boldsymbol{\tau}(\mathbf{r}, t) = \boldsymbol{\tau}(\mathbf{r}, t)$ and $\delta Q_{ij}(\mathbf{r}, t) = Q_{ij}(\mathbf{r}, t) - Q_{ij}^0$. We will generally work in Fourier space by introducing Fourier transforms of the fluctuations as $\phi_{\mathbf{k}}^\alpha(t) = \int_{\mathbf{r}} e^{i\mathbf{k}\cdot\mathbf{r}} \delta\phi_\alpha(\mathbf{r}, t)$, where $\delta\phi_\alpha = (\delta\rho, \boldsymbol{\tau}, \delta Q_{ij})$.

3.1 Dynamical self-regulation and banding instability

We first consider the linear dynamics of the system in the region just above the mean-field transition at ρ_c . For simplicity we only discuss spatial variations normal to the direction of broken symmetry, as these correspond to the most unstable modes, *i.e.*, let $\mathbf{k} = k\hat{\mathbf{y}}$. Fluctuations in τ_x and δQ_{xy} then decouple and are always stable. The dynamics of fluctuations in $\delta\rho$, τ_y and δQ_{yy} is governed by three coupled equations. Fluctuations in τ_y are always quickly damped near the mean-field transition, while the decay rate of δQ_{yy} , controlled to leading order by α_0 , vanishes as $\rho_0 \rightarrow \rho_c^+$. We therefore neglect fluctuations in τ_y and simply examine the coupled dynamics of $\delta\rho$ and $\delta Q \equiv \delta Q_{yy}$, given by

$$\partial_t \delta\rho_{\mathbf{k}} = -k^2 \delta\rho_{\mathbf{k}} - \bar{D}_Q k^2 \delta Q_{\mathbf{k}}, \quad (5a)$$

$$\begin{aligned} \partial_t \delta Q_{\mathbf{k}} = - \left[\frac{\alpha_0}{2} + (1 + \bar{D}_s) k^2 \right] \delta Q_{\mathbf{k}} \\ - \frac{1}{2} (\alpha' Q_0 + \bar{D}_\rho k^2) \delta\rho_{\mathbf{k}}, \end{aligned} \quad (5b)$$

where $\alpha' = \left(\frac{\partial\alpha}{\partial\rho} \right)_{\rho=\rho_0}$, or $\alpha' = 1/\rho_c$ with the chosen parameters. The decay of density and ordered parameter fluctuations is then controlled by two coupled hydrodynamic modes. One of the modes has a finite decay rate (proportional to α_0) in the limit $k \rightarrow 0$ and is always stable. At small wave vector, the dispersion relation of the other mode is given by

$$s_y(k) = -s_2 k^2 - s_4 k^4 + \mathcal{O}(k^6), \quad (6)$$

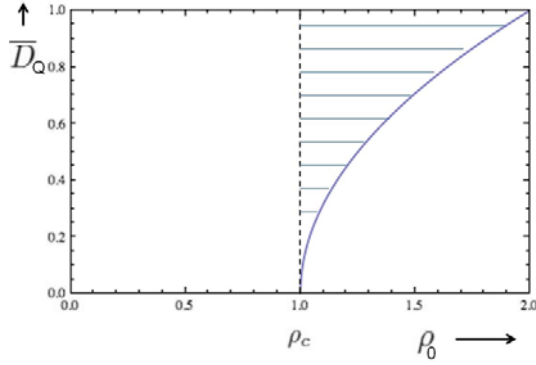


Fig. 3. The banding instability that occurs due to the self-regulating nature of the flow. The dashed vertical line indicates the mean-field order-disorder transition at $\rho_0 = \rho_c$. The solid line (blue online) is the boundary of the instability, corresponding to $s_2 = 0$ (see eq. (6)), or $\bar{D}_Q = \mathcal{D}_Q/D_0 = \sqrt{\alpha_0\beta}/\alpha'$. The plot is for $\alpha_0 = \rho_0/\rho_c - 1$, $\alpha' = 1/\rho_c$ and $\beta = 1 + \rho/\rho_c$, with the choice $\rho_c = 1$. The uniform ordered state is unstable in the striped region.

with $s_2 = 1 - \frac{\bar{D}_Q\alpha'}{\sqrt{\alpha_0\beta}}$ and $s_4 > 0$. Near the transition where $\alpha_0 \rightarrow 0$, $s_2 < 0$ and $s_4 \simeq \frac{2\bar{D}_Q^2\alpha'^2}{\alpha_0^2\beta}$. As a result, $s_y(k) > 0$ for a range of wave vectors, resulting in the unstable growth of density and order parameter fluctuations illustrated in fig. 3. The fastest growing mode has wave vector $k_0 = \sqrt{-s_2/2s_4} \sim (\rho_0 - \rho_c)^{3/2}$. Including the coupling to τ_y will yield finite Peclet number corrections to the instability. Note that this instability is strongest in the vicinity of the order-disorder transition and is a manifestation of the fact that the dynamics of the system is self-regulating, *i.e.*, the control parameter associated with the phase transition, namely the density is dynamically coupled to the emergent ordering that results from the transition through the curvature-induced fluxes. This is the dynamics that leads the system to be intrinsically phase separated [3].

We recall that polar active fluids exhibit a similar instability for wave vectors parallel to the direction of mean order. In that case the mode that goes unstable is a propagating mode and the instability signals the onset of solitary waves consisting of alternating ordered and disordered bands extending in the direction normal to that of mean order and traveling along the direction of broken symmetry. These bands have been observed in simulations of the Vicsek model [13, 40], as well as in numerical solutions of the nonlinear hydrodynamic equations for polar fluids [41–43]. We have shown here that active nematics exhibit a similar instability, controlled by the interplay of curvature currents (\bar{D}_Q) and the self-regulation due to the density dependence of α . The instability occurs even for $\bar{v} = 0$, *i.e.*, is present in both active and self-propelled nematics. It occurs for wave vectors perpendicular to the direction of broken nematic symmetry and the mode that goes unstable is a diffusive one. It is therefore tempting to associate it with the emergence of the stationary bands consisting of alternating ordered (nematic) and disorders

regions that have been seen in simulations of active systems with apolar interactions [33] and physical excluded-volume interactions [34, 36]. Finally, but most importantly, this instability mechanism is *generic*, in the sense that it does not depend on microscopic parameters, but only on the presence of a dynamical feedback between density and active currents.

3.2 Curvature-induced flux

Next we consider the region of small \bar{v} , λ and γ , deep in the nematic phase. In this case, the long-wavelength dynamics is controlled by hydrodynamic modes associated with fluctuations in the density and the director $\hat{\mathbf{n}}$. This case has been considered in the literature already and is summarized here for completeness [3, 30, 44]. For our choice of coordinates to linear order we have $\delta Q_{xx} = -\delta Q_{yy} = 0$ and $\delta Q_{xy} = \delta Q_{yx} = Q_0\delta\hat{n}(\mathbf{r}, t)$. Neglecting polarization fluctuations that decay on microscopic time scales, the linearized equations are given by

$$\partial_t\delta\rho_{\mathbf{k}} = -k^2\delta\rho_{\mathbf{k}} - Q_0\bar{D}k^2\sin 2\theta\delta\hat{n}_{\mathbf{k}}, \quad (7a)$$

$$\partial_t\delta\hat{n}_{\mathbf{k}} = -\frac{\bar{D}_\rho k^2}{2Q_0}\sin 2\theta\delta\rho_{\mathbf{k}} + [\bar{D}_s + \cos 2\theta]k^2\delta\hat{n}_{\mathbf{k}}, \quad (7b)$$

where θ is the angle between \mathbf{k} and the direction of broken symmetry (x). If $\theta = 0, \pi$, the two equations are decoupled and the modes are diffusive and stable. For general θ one of the hydrodynamic modes becomes unstable for $\bar{D}\bar{D}_\rho\sin^2 2\theta > 2(\bar{D}_s + \cos 2\theta)$. This can be satisfied provided $\bar{D}_Q\bar{D}_\rho > 2D_s$, *i.e.*, the curvature-driven fluxes exceed the restoring effects of diffusion. This instability has been discussed in detail elsewhere [30].

3.3 Induced polar order

Finally, we examine the effect of fluctuations with spatial variations along the direction of broken symmetry, *i.e.*, $\mathbf{k} = k\hat{\mathbf{x}}$. The relevant coupled fluctuations in this case are $\delta\rho$, τ_x and δQ_{xx} . For simplicity, we consider the regime of large Peclet number \bar{v} , where the linear dynamics is controlled by Euler order terms and neglect terms quadratic in the gradients, with the result

$$\partial_t\delta\rho_{\mathbf{k}} + ik\bar{v}\tau_{x,\mathbf{k}} = 0, \quad (8)$$

$$\partial_t\tau_{x,\mathbf{k}} + \gamma_e\tau_{x,\mathbf{k}} = -ik\bar{v}\delta Q_{xx,\mathbf{k}} - ik\frac{\bar{v}}{2}\delta\rho_{\mathbf{k}}, \quad (9)$$

$$\partial_t\delta Q_{xx,\mathbf{k}} - \frac{\alpha_0}{2}\delta Q_{xx,\mathbf{k}} = ik\left(\bar{v} + \frac{\lambda}{2}Q_0\right)\tau_{x,\mathbf{k}} + \frac{\alpha'}{2}Q_0\delta\rho_{\mathbf{k}}, \quad (10)$$

where $\gamma_e = 1 + \frac{\gamma}{2}Q_0^2 - \frac{\gamma}{2}Q_0$. As discussed earlier and highlighted in fig. 2, the anisotropy of small angle collisions in the nematic state enhances polar order by suppressing the decay rate of $\tau_{x,\mathbf{k}}$ from its bare value of 1 (in units of D_r^{-1}) to γ_e . The dispersion relations of the hydrodynamic modes associated with eqs. (6) are easily calculated at small wave

vectors. The diffusive mode associated with the density fluctuations (the only hydrodynamic mode proper here) is given by

$$s_x(k) = -k^2 \frac{\bar{v}^2}{2\gamma_e} \left(1 + \frac{2\alpha'}{\sqrt{\alpha_0\beta}} \right) \quad (11)$$

and becomes unstable when $\gamma_e \leq 0$. It is also evident that if $\gamma_e \leq 0$ the polarization fluctuations no longer decay. In general γ_e depends on microscopic details of the model, but there is no reason to exclude *a priori* that it could change sign and indeed does for the case of long thin hard rods with excluded-volume interactions [30]. The linear analysis here is of limited utility because of the existence of a homogeneous instability but it is shown to indicate that the build up of polarization due to the momentum-conserving nature of the interactions has a dramatic consequence on the dynamics of the system. We stress that the instability discussed in this section is associated with the polarization, not with the nematic order parameter. Simulations of self-propelled hard rods have seen ubiquitously traveling clusters of aligned rods [34, 35] that also seem to exhibit a layered or smectic structure within the cluster [34, 36]. Given our calculation indicates an instability of polar order in the longitudinal direction, it is tempting to speculate that this instability may be the indication of the formation of the smectic layers seen in simulations.

Finally, we stress that the nonlinear homogeneous terms proportional to γ and responsible for the renormalization of γ_e always vanish in an equilibrium state because the nematic symmetry of such a state by definition forbids a nonzero uniform value of the mean polarization.

4 Discussion

We have considered in this paper the hydrodynamics of active overdamped fluids that can order in nematic states. These are collections of active particles that interact via apolar (nematic) aligning interactions, such as steric repulsion or medium-mediated hydrodynamic couplings. One can identify two classes of such fluids, depending on the properties of the individual active units. Active nematics consist of shaker particles that are themselves apolar. Self-propelled nematics are collections of particles that are physically head-tail symmetric (such as SP rods), but where a microscopic dynamical polarity is induced by self-propulsion. Although both systems form ordered states of nematic symmetry, their dynamical behavior is qualitatively different, as seen in recent simulations [34, 35, 38].

The hydrodynamic equations of active nematics have the form given in eqs. (2). We have shown that the same equations are also obtained by considering SP particles and neglecting the effect of self-propulsion on the interaction between active units, suggesting that the active nematic may be considered the zero Peclet number \bar{v} limit of self-propelled nematic. In this case the only active term is the curvature current proportional to \mathcal{D}_Q in eq. (2a). This nonequilibrium coupling of orientation and flow induces

instabilities of the ordered state that have been studied before in the literature [3, 14, 30] and are also summarized in sect. 3.2. The curvature current is also key in controlling the banding instability arising from dynamical self-regulation discussed in sect. 3.1. In fact this instability, although not discussed before in the literature for overdamped active nematic, occurs in all active fluids of nematic symmetry, both for shakers and self-propelled particles. It arises from the density dependence of the parameter $\alpha(\rho)$ that controls the mean-field transition and the fact that in active systems ρ is not tuned from the outside, as in equilibrium, but is itself a dynamical variable convected by the order parameter.

The hydrodynamic equations of self-propelled nematics given in eqs. (3) (or eqs. (4) in the dimensionless form studied here) contain many new active terms that arise from modifications of the two-body interaction due to self-propulsion. These equations have also been derived by us for a specific microscopic model of self-propelled hard rods [15, 39], although the low order closure of the kinetic theory used in that work only gives terms up to quadratic in the hydrodynamic fields. Self-propelled nematics also exhibit both the curvature-induced instability discussed in sect. 3.2 and the banding instability discussed in sect. 3.1. Both are of course modified at finite Peclet number due to additional convective contributions to the underlying mechanisms the details of which will be discussed elsewhere. In addition, self-propulsion yields a novel instability due to the built-up of local polar order discussed in sect. 3.3. This arises because in the nematic state most binary collisions involve nematogens that are nearly aligned or anti aligned, as shown in fig. 2. When the nematogens are self-propelled, collisions of nearly aligned and nearly anti-aligned pairs are not identical. Nearly aligned pairs tend to further align upon collisions, while nearly anti-aligned pairs are turned away from each other. As a result, local polar order is enhanced and the nematic state becomes unstable as discussed in sect. 3.3. It is tempting to associate this instability with the onset of ‘‘polar clusters’’ that have been observed ubiquitously in simulations of self-propelled rods [34, 35, 38], as well as in experiments in gliding myxobacteria [17].

MCM was supported by the National Science Foundation through awards DMR-0806511 and DMR-1004789. AB was supported by the Brandeis-MRSEC through NSF DMR-0820492.

References

1. J. Toner, Y. Tu, Phys. Rev. Lett. **75**, 4326 (1995).
2. J. Toner, Y. Tu, Phys. Rev. E **58**, 4828 (1998).
3. S. Ramaswamy, R.A. Simha, J. Toner, Europhys. Lett. **62**, 196 (2003).
4. V. Narayan, S. Ramaswamy, N. Menon, Science **317**, 105 (2007).
5. A.J. Koch, H. Meinhardt, Rev. Mod. Phys. **66**, 1481 (1994).
6. E. Budrene, H. Berg, Nature **349**, 630 (1991).

7. E.O. Budrene, H. Berg, *Nature* **376**, 49 (1995).
8. M. Matsushita, in *Bacteria as Multicellular Organisms*, edited by J.A. Shapiro, M. Dworkin (Oxford University Press, 1997).
9. S. Ramaswamy, *Annu. Rev. Condens. Matter Phys.* **1**, 323 (2010).
10. H. Gruler, U. Dewald, M. Eberhardt, *Eur. Phys. J. B* **11**, 187 (1999).
11. R. Kemkemer, D. Kling, D. Kaufmann, H. Gruler, *Eur. Phys. J. E* **1**, 215 (2000).
12. T. Vicsek, A. Czirók, E. Ben-Jacob, I. Cohen, O. Shochet, *Phys. Rev. Lett.* **75**, 1226 (1995).
13. G. Grégoire, H. Chaté, *Phys. Rev. Lett.* **92**, 025702 (2004).
14. A. Simha, S. Ramaswamy, *Phys. Rev. Lett.* **89**, 058101 (2002).
15. A. Baskaran, M.C. Marchetti, *Phys. Rev. Lett.* **101**, 268101 (2008).
16. A. Baskaran, M.C. Marchetti, *Proc. Natl. Acad. Sci. U.S.A.* **106**, 15567 (2009).
17. F. Peruani, J. Starruss, V. Jakovljevic, L. Sogaard-Anderseng, A. Deutsch, M. Bär, *Phys. Rev. Lett.* **108**, 098102 (2012).
18. J. Palacci, B. Abécassis, C. Cottin-Bizonne, C. Ybert, L. Bocquet, *Phys. Rev. Lett.* **104**, 138302 (2010).
19. A. Saez, M. Ghibaudo, A. Buguin, P. Silberzan, B. Ladoux, *Proc. Natl. Acad. Sci. U.S.A.* **104**, 8281 (2007).
20. L. Petitjean, M. Reffay, E. Grasland-Mongrain, M. Pouxjade, B. Ladoux, A. Buguin, P. Silberzan, *Biophys. J.* **98**, 1790 (2010).
21. K. Kruse, F. Joanny, F. Jülicher, J. Prost, K. Sekimoto, *Phys. Rev. Lett.* **92**, 078101 (2004).
22. R. Voituriez, J.F. Joanny, J. Prost, *Europhys. Lett.* **70**, 404 (2005).
23. R. Voituriez, J.F. Joanny, J. Prost, *Phys. Rev. Lett.* **96**, 28102 (2006).
24. D. Marenduzzo, E. Orlandini, J.M. Yeomans, *Phys. Rev. Lett.* **98**, 118102 (2007).
25. L. Giomi, M.C. Marchetti, T. Liverpool, *Phys. Rev. Lett.* **101**, 198101 (2008).
26. M.E. Cates, S.M. Fielding, D. Marenduzzo, E. Orlandini, J.M. Yeomans, *Phys. Rev. Lett.* **101**, 068192 (2008).
27. A. Sokolov, I.S. Aranson, *Phys. Rev. Lett.* **103**, 148101 (2009).
28. L. Giomi, T.B. Liverpool, M.C. Marchetti, *Phys. Rev. E* **81**, 051908 (2010).
29. D. Saintillan, *Phys. Rev. E* **81**, 056307 (2010).
30. A. Baskaran, M.C. Marchetti, *Phys. Rev. E* **77**, 011920 (2008).
31. A. Gopinath, M.F. Hagan, M.C. Marchetti, A. Baskaran, *Phys. Rev. E* **85**, 061903 (2012).
32. J. Toner, Y. Tu, S. Ramaswamy, *Ann. Phys.* **318**, 170 (2005).
33. H. Chaté, F. Ginelli, R. Montagne, *Phys. Rev. Lett.* **96**, 180602 (2006).
34. Y. Yang, V. Marceau, G. Gompper, *Phys. Rev. E* **82**, 031904 (2010).
35. F. Ginelli, F. Peruani, M. Bär, H. Chaté, *Phys. Rev. Lett.* **104**, 184502 (2010).
36. S.R. McCandlish, A. Baskaran, M.F. Hagan, *Soft Matter* **8**, 2527 (2012).
37. M.E. Cates, D. Marenduzzo, I. Pagonabarraga, J. Tailleur, *Proc. Natl. Acad. Sci. U.S.A.* **107**, 11715 (2010).
38. F. Peruani, A. Deutsch, M. Bär, *Phys. Rev. E* **74**, 030904 (2006).
39. A. Baskaran, M.C. Marchetti, *J. Stat. Mech: Theor. Exp.*, P04019 (2010).
40. H. Chaté, F. Ginelli, G. Grégoire, F. Peruani, F. Raynaud, *Eur. Phys. J. B* **64**, 451 (2008).
41. E. Bertin, M. Droz, G. Grégoire, *Phys. Rev. E* **74**, 022101 (2006).
42. E. Bertin, M. Droz, G. Grégoire, *J. Phys. A: Math. Theor.* **42**, 445001 (2009).
43. S. Mishra, A. Baskaran, M.C. Marchetti, *Phys. Rev. E* **81**, 061916 (2010).
44. R.A. Simha, S. Ramaswamy, *Physica A* **306**, 262 (2002).